Prediction of Intermediate Crack Debonding Strain of Externally Bonded FRP Laminates in RC Beams and One-Way Slabs

H. M. Elsanadedy[1]; H. Abbas, M.ASCE[2]; Y. A. Al-Salloum[3]; and T. H. Almusallam[4]

Abstract: Interface crack propagation of FRP (fiber-reinforced polymer) strengthened reinforced concrete (RC) flexural member is often initiated from the toes of the intermediate cracks and propagates towards the supports. This type of FRP delamination is commonly termed intermediate crack (IC) debonding and is common for flexural members with high shear span-to-depth ratios. If the ultimate FRP strain at IC debonding failure is known, the moment capacity of the member can be obtained through a simple section analysis. This research deals with the prediction of ultimate FRP strain at IC debonding, using neural networks and regression models. Basic information on neural networks and the types of neural networks most suitable for the analysis of experimental results are given. A set of experimental data for FRP-strengthened RC beams and one-way slabs, covering a large range of parameters, for the training and testing of neural networks is used. The available test results were not only compared with current code provisions but with equations proposed by other researchers as well. The prediction models based on neural network are presented. A new design equation is also suggested. **DOI: 10.1061/(ASCE)CC.1943-5614.0000462.** © *2014 American Society of Civil Engineers.*

Author keywords: FRP; Concrete beams; Concrete slabs; External strengthening; Debonding; ANN (artificial neural network).

Introduction

Among several methods available for strengthening of reinforced concrete (RC) beams and slabs, the application of externally bonded fiber-reinforced polymer (FRP) composites has received significant attention from the rehabilitation community. Advantages of FRP composites include: high strength-to-weight ratio, ease of installation, non-corrosive characteristic, strong resistance to environment and fatigue, and reduced long-term maintenance costs (Bakis et al. 2002; Teng et al. 2003). FRP fabrics or laminates may be bonded to the tension soffit of RC beams or slabs to improve their load-carrying capacity. Such a rehabilitation method has been extensively studied from laboratory-scale research to full-scale field applications (Lopez and Nanni 2006; Kim et al. 2008a).

For FRP-upgraded flexural members, depending on the combination of parameters such as member size, steel reinforcement ratio, FRP properties and dimensions, failure may occur in different modes (Meier 1995; Arduini et al. 1997; Buyukozturk and Hearing 1998). The dominant failure mode is debonding of the FRP system. Debonding failure typically propagates within the concrete substrate. Sources of FRP debonding include local cracks in a host concrete beam, degradation of FRP-concrete interface and stress concentrations induced by FRP configurations and irregular concrete surface (Smith and Teng 2001; Mazzotti et al. 2008). Most FRP-debonding may be classified (Oehlers et al. 2003) as either end-peeling or intermediate-crack-induced debonding (*IC debonding* henceforth). End-peeling occurs owing to the combination of normal and shear stresses at the termination point of FRP and propagates along the FRP. IC debonding is induced by a geometric discontinuity of a strengthened member at the location of flexural or shear/flexural cracks and propagates in the direction of decreasing moment. End-peeling failure usually propagates at the level of the internal reinforcement (splitting-like failure), whereas IC debonding takes place within the concrete cover a few mm above the bond line. IC debonding limits the composite behavior and therefore influences the effectiveness of the FRP system. Local debonding failure propagates along the FRP-concrete interface zone with increased load. In practice, end peeling is easily mitigated using anchorage (typically, FRP U-wraps) near the termination point of FRP. IC debonding is not easily controlled (Sebastian 2001; Kim et al. 2008b) and therefore FRP stresses must be limited to mitigate it.

Knowing the FRP strain at debonding failure, a conventional section analysis similar to that for normal RC members can be performed. Based on the equilibrium of axial forces in the FRP, steel and concrete, the position of the neutral axis is obtained. The moment capacity of the strengthened member can hence be determined. Various design models are available for predicting IC debonding strain of FRP-strengthened members; many have limited applicability and most are empirical in nature (e.g., Said and Wu 2008; Wu et al. 2009). However, a method that is fully verified with experiments and universally accepted by the research and design communities is yet to appear.

In recent years, artificial neural networks (ANNs) have been of interest to researchers in the modeling of various civil engineering systems. The IC debonding strain of FRP-strengthened flexural members is affected by unknown multivariable interrelationships and the existing experimental data are noisy; consequently, the

[1]Assistant Professor, Dept. of Civil Engineering, King Saud Univ., Riyadh 11421, Saudi Arabia.

[2]Professor, Specialty Units for Safety and Preservation of Structures, Dept. of Civil Engineering, King Saud Univ., Riyadh 11421, Saudi Arabia (corresponding author). E-mail: abbas_husain@hotmail.com

[3]Professor, Dept. of Civil Engineering, King Saud Univ., Riyadh 11421, Saudi Arabia.

[4]Professor, Dept. of Civil Engineering, King Saud Univ., Riyadh 11421, Saudi Arabia.

Note. This manuscript was submitted on August 24, 2013; approved on December 9, 2013; published online on February 19, 2014. Discussion period open until July 19, 2014; separate discussions must be submitted for individual papers. This paper is part of the ***Journal of Composites for Construction***, © ASCE, ISSN 1090-0268/04014008(16)/$25.00.

models derived by regression analysis may not predict the behavior well. The ANN automatically manages the relationships between variables and adapts based on the data used for their training. So, it is important to collect a large number of experimental data. In this study, a large test database, built from an extensive survey of existing tests on FRP-upgraded beams and one-way slabs, is carefully examined to establish the effect of various variables. Finally, a new model is proposed based on ANN for the prediction of IC debonding strain. A regression-based model has also been developed for the prediction of IC debonding strain of FRP-strengthened members. The test results were compared with the results predicted by ANN and the regression models. A new design equation is also suggested.

Existing Models and Code Provisions for IC Debonding

Most existing models consider the bond capacity of FRP sheets in terms of the maximum transferable load (Smith and Teng 2002; Karbhari et al. 2006; Toutanji et al. 2007). IC debonding (or effective) strains, however, are more appropriate to use in practice because these are easily calculated in plane-sections analysis, which assumes that the plane section before bending remains plane after bending and full-interaction/perfect bond exists between materials. ACI 440.2R-08 (ACI Committee 440 2008) recommends the effective strain of FRP be limited to the strain at which debonding may occur. Tables 1 and 2 enlist design models, adopted by some selected existing codes of standards and researchers, which estimate the IC debonding strain of FRP sheets. It should be noted that the tensile strength of concrete (f_{ct}) is calculated, wherever required, using Eq. (1) that is equivalent to the modulus of rupture prescribed by ACI 318-11 (ACI Committee 318 2011).

$$f_{ct} = 0.62\sqrt{f'_c} \quad (1)$$

where f'_c is the specified compressive strength of concrete in MPa.

The Experimental Database

To provide sufficient information to train and verify the neural network and to develop a regression model, a comprehensive set of data has to be collected. An extensive review of the literature was therefore conducted to compile a database of test results on FRP-strengthened RC beams and one-way slabs that fail in IC debonding. The database comprises of 149 rectangular beams, 23 T-beams and 31 one-way slabs. Altogether, 203 test results were collected from 62 experimental programs carried out between 1991 and 2012, as summarized in Tables 3–5. The experimental tests selected from the literature were those for which most material and geometric characteristics were clearly reported. To assemble a consistent database, the following criteria were used:

- All beams and slabs are conventionally reinforced with steel rebars and strengthened with constant-thickness carbon, glass or aramid FRP sheets.
- Failure of the specimens was due to IC debonding.

Table 1. Models Provided by Different Codes and Standards for IC Debonding Strain

Code	IC debonding strain of FRP reinforcement (ε_{fd}) (Units: N and mm)
ACI 440.2R-08 (2008)	$\varepsilon_{fd} = 0.41\sqrt{f'_c/nE_f t_f} \le 0.9\varepsilon_{fu}$
JSCE Recommendations (2001)	$\varepsilon_{fd} = \sqrt{2G_f/nE_f t_f}$ where G_f is the fracture energy of the FRP-concrete interface. Given that the interfacial fracture energy is not readily determined without experimental work, Wu and Niu (2007) suggested an empirical equation that can be used with the JSCE model: $G_f = 0.644(f'_c)^{0.19}$
Concrete Society TR55 (2004)	$\varepsilon_{fd} = 0.5k_b\sqrt{f_{ct}/nE_f t_f}$ where $k_b = 1.06\sqrt{(2-b_f/b)/(1+b_f/400)} \ge 1.0$ with $b_f/b \ge 0.33$
CNR DT-200 R1/2012 (NRC 2012)	$\varepsilon_{fd} = 0.373\sqrt{k_b\sqrt{f_{ct}f'_c}/nE_f t_f}$ (for a typical design case) where $k_b = \sqrt{(2-b_f/b)/(1+b_f/b)} \ge 1.0$ with $b_f/b \ge 0.25$
Chinese Code CECS-146 (2003)	$\varepsilon_{fd} = k_b f_{ct}[(1/\sqrt{nE_f t_f}) - (0.2/L_d)]$ where $k_b = \sqrt{(2.25-b_f/b)/(1.25+b_f/b)}$

Note: b = width of concrete section; b_f = width of FRP sheet; E_f = tensile modulus of elasticity of FRP; f'_c = specified compressive strength of concrete; f_{ct} = tensile strength of concrete, calculated using Eq. (1); L_d = FRP distance from its end to the section where it is fully utilized; n = number of plies of FRP reinforcement; t_f = thickness of one ply of FRP reinforcement.

Table 2. Models Proposed by Different Researchers for IC Debonding Strain

Researcher	IC debonding strain of FRP reinforcement (ε_{fd}) (Units: N and mm)
Teng et al. (2003)	$\varepsilon_{fd} = 0.48k_b k_L\sqrt{\sqrt{f'_c}/nE_f t_f}$ where $k_b = \sqrt{(2-b_f/b)/(1+b_f/b)}$ and $k_L = \begin{cases} 1 & \text{if } L_d \ge L_e \\ \sin\frac{\pi L_d}{2L_e} & \text{if } L_d < L_e \end{cases}$ in which L_e is the effective bond length given by: $L_e = \sqrt{nE_f t_f/\sqrt{f'_c}}$
Lu et al. (2007)	$\varepsilon_{fd} = 1.5k_b f_{ct}[(0.503/\sqrt{nE_f t_f}) - (0.0886/L_d)]$ where $k_b = \sqrt{(2.25-b_f/b)/(1.25+b_f/b)}$
Said and Wu (2008)	$\varepsilon_{fd} = 0.23(f'_c)^{0.2}/(nE_f t_f)^{0.35}$
Bilotta et al. (2013)	$\varepsilon_{fd} = k_{1C}/\gamma_{f,d} \cdot FC\sqrt{2k_b\sqrt{f'_c f_{ct}}/nE_f t_f}$ where k_{1C} is a coefficient calibrated on experimental results and it can be conservatively taken as 0.18; $\gamma_{f,d}$ is a safety factor based on the level of quality control in the FRP application and it can be taken as 1.2; FC is the confidence factor based, in principle, on the level of knowledge achieved on the existing material properties and it can be conservatively taken as $\sqrt{1.5}$ and $k_b = \sqrt{(2-b_f/b)/(1+b_f/b)} \ge 1.0$ with $b_f/b \ge 0.25$

Note: b = width of concrete section; b_f = width of FRP sheet; E_f = tensile modulus of elasticity of FRP; f'_c = specified compressive strength of concrete; f_{ct} = tensile strength of concrete, calculated using Eq. (1); L_d = FRP distance from its end to the section where it is fully utilized; n = number of plies of FRP reinforcement; t_f = thickness of one ply of FRP reinforcement.

Table 3. Sources of the Experimental Database of Rectangular Beams

Reference	Specimen designation	Number of test data
Al-Zaid et al. (2010)	B-II-1	1
Al-Negheimish et al. (2011)	B-II-2, B-II-3, B-II-5	3
Breña et al. (2003)	A3, A4, B1, C1, C2, D2	6
Matthys (2000)	BF2, BF3, BF4-Prc, BF5-Sus, BF8, BF9	6
Bonacci and Maalej (2000)	B2, B3-Sus	2
Kotynia (2005)	B-04/0.5S, B-08/S1, BF-04/0.55, BF-06/S	4
Reeve (2005)	H1, H2, H2x1, H4, L1, L2, L2x1, L4	8
Grace et al. (2002)	H-75-2, C-3	2
Maalej and Leong (2005)	A3, A4, A5, A6, B3, B4, B5, B6, C3, C4	10
Ceroni (2010)	A2	1
Saadatmanesh and Ehsani (1991)	B	1
Kaminska and Kotynia (2000)	BO-08/S	1
Rahimi and Hutchinson (2001)	B3, B6	2
Fang (2002)	B1, B2, B3	3
Kotynia and Kaminska (2003)	B-08S, B-08M	2
Zhang et al. (2003)	A-AK, B-C1, B-AT, B-AK	4
Dias et al. (2004)	V2, V4	2
Khomwan et al. (2004)	B2, B6	2
Quattlebaum et al. (2005)	C-S	1
Breña and Macri (2004)	A1-I, A1-II, A2-I, A3-I, A3-II, A4-I, A4-II, A5-I, A5-II, C1-Iia, C1-IIb	11
Kurtz et al. (2008)	2, 10, 20, 22, 27, 28	6
Kurtz and Balaguru (2001)	OS	1
Lee and Moy (2007)	B11, B12, B21, B22, B31, B32	6
Pham and Al-Mahaidi (2006)	S1a, S1b, S2a, S2b, S3a, S3b	6
Rusinowski and Täljsten (2009)	Beam 2, Beam 6	2
Ai-hui et al. (2006)	A10, A20, B10, B20	4
Bakay et al. (2009)	1, 4, 2, 3, 9, 10, 11, 12, 5, 6	10
Neagoe (2011)	B-01, B-02, B-03, B-04	4
Gunes et al. (2009)	S2PF7M, S3PS1M, S3PS2M	3
Farah and Sato (2007)	SP-C1, SP-C2	2
Alagusundaramoorthy et al. (2002)	CB3-2S, CB5-3S, CB6-3S, CB7-1S, CB8-1SB, CB9-1SB, CB10-2SB, CB13-2F	8
Fanning and Kelly (2001)	F3	1
Grace et al. (2003)	F-CB-1	1
Arduini and Nanni (1997)	SM2, SM3, MM2, MM3	4
Pan et al. (2010)	B5, B6, B7, B8	4
Grace and Singh (2005)	B-P, B-F	2
David et al. (1998)	P7	1
White et al. (2001)	S-A, R-A	2
You et al. (2012)	NFCB1, NFCBW2	2
Bsisu et al. (2012)	B-CFRP	1
Chahrour and Soudki (2005)	Beam 2	1
GangaRao and Vijay (1998)	7A-C	1
Sena-Cruz et al. (2012)	EBR	1
Spadea et al. (2001)	A1.1, A3.1	2
Juvandes (1999)	B.3, B.7	2
Total number of specimens		149

- The FRP sheet was neither prestressed nor anchored in any form at its ends.
- The specimens did not experience prior cyclic loading after being strengthened with FRP and before being tested statically to debonding failure.
- Only specimens with reported IC debonding strain were used.
- Sufficient details about various geometric and material parameters were provided to enable the use of the results with confidence.

The database contains some subsets of two to three data with the same material and geometrical parameters. These subsets cannot be averaged for the loss of variability within the subsets because of the replacement of many members of a subset by one member representing their average. Thus, the data have been used in the present analysis without any modification.

The histograms of the raw variables' data used in the analysis are shown in Figs. 1–6. SD and CV in these figures stand for standard deviation and coefficient of variation, respectively. The minimum and maximum values of the variables are mentioned in the first and last range of variables on the x-axis. The data are sorted in six bins of almost uniform width. The number of bins is taken as the cube root of the number of data points. The observations made from these figures are:

1. Though the ratio of the width of FRP sheet to the width of concrete section (i.e., b_f/b) varies from 0.073–1.0 thus covering from very narrow strips to the strips covering full width of sections but large amount of data (36.5%) is for width of strip close to the width of concrete section (Fig. 1).
2. The yield strain of steel rebars varies from 0.14–0.34% (Fig. 2). The data for high yield strain range of 0.30–0.34% are quite low (2.0%).
3. The value of nt_fE_f, representing the axial rigidity of FRP sheets, varies from 16–580 kN/mm, but most of the data (96.6%) is for the range of 16–580 kN/mm (Fig. 3). The bin of 16–100 kN/mm range contains the maximum data (45.8%).
4. Though the percentage of steel rebars varies from 0.15–3.6%, but most of the data (99%) is for the 0.15–1.8% range (Fig. 4). The bin containing majority of data (47.8%) is for the percentage of rebars varying from 0.6–1.25%.
5. Though the compressive strength of concrete ranges from very low (12.64 MPa) to high (80 MPa), but most of the data (94.1%) is for the 20–60 MPa range (Fig. 5). Maximum data (36.9%) are for compressive strength of concrete varying from 30–40 MPa. The data for high strength concrete (>42 MPa) are 34.0%.
6. There is wide range of modulus of elasticity (Fig. 6) because of varied materials covered in the database which is consisting of carbon, glass and aramid. The modulus of elasticity of FRP varies from 20–271 GPa, with most of the data (73.9%) lying in the ranges of 140–180 and 220–271 GPa.

The histogram of IC debonding strain (i.e., output) is plotted in Fig. 7. It is observed from the figure that the IC debonding strain varies from 0.38–1.5%, and the bin of 0.5–0.7% strain range contains maximum data (50.2%).

Neural Network Models

The FRP-debonding in FRP-strengthened flexural RC members at failure is a complex nonlinear process dependent on many variables; it is a problem well suited to the ANNs. In the last few years, the ANN approach, a subfield of artificial intelligence, has been used to solve a wide variety of problems in civil engineering

Table 4. Sources of the Experimental Database of T-beams

Reference	Specimen designation	Number of test data
Yalim et al. (2008)	W-CSP1-0, W-CSP1-0E, W-CSP1-4(1), W-CSP1-4(3), W-CSP2-3-0, W-CSP2-3-4(1), W-CSP2-3-4(2), W-CSP2-3-4(3), W-CSP6-9-0, W-CSP6-9-4(1), W-CSP6-9-4(2), W-CSP6-9-4(3), P-CSP1(1), P-CSP2-3(1), P-CSP2-3(2), P-CSP6-9(1), P-CSP6-9(2)	17
Park (2001)	No.3, No. 4, No. 6, No. 7	4
Salib (2012)	B2	1
Cameron (2012)	EB1	1
Total number of specimens		23

Table 5. Sources of the Experimental Database of One-Way Slabs

Reference	Specimen designation	Number of test data
Yao et al. (2005)	III-1, III-2, III-4	3
Ye et al. (2001)	BM0	1
Seim et al. (2001)	S12	1
Al-Rousan et al. (2012)	G2-1	1
Smith et al. (2011)	S2	1
Gao et al. (2011)	CFRP-1, CFRP-2, CFRP-3, GFRP-1, GFRP-2, GFRP-3	6
Yao et al. (2002)	CP1, CP2, CP3, CP4, CP5, CS1, CS2, GS1, GS2	9
Smith and Kim (2009)	Slab 6	1
Kotynia et al. (2011)	G2	1
Ramanathan (2008)	4 × 1	1
Napoli (2008)	EB	1
Tan (2003)	A	1
Azevedo et al. (2005)	LC2S, LB2S, LD4BL, LE4I	4
Total number of specimens		31

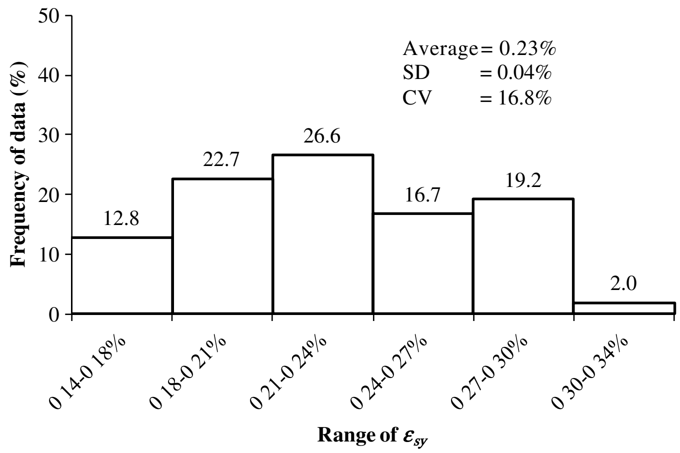

Fig. 2. Frequency distribution of the yield strain of rebars

applications (Adhikary and Mutsuyoshi 2006; Elsanadedy et al. 2012; Shah et al. 2012; Topcu and Saridemir 2008). The most important property of ANN in civil engineering problems is their capability of learning directly from examples.

The manner in which the data are presented for training is the most important aspect of the neural network method. Often this can be done in more than one way; the best configuration being determined by trial-and-error. It can also be beneficial to examine the input/output patterns or data sets that the network finds difficult to learn. This enables a comparison of the performance of the neural network model for these different combinations of data. To map the causal relationship related to the IC debonding strain of FRP-strengthened RC members, two separate input/output schemes (called Model-A1 and Model-A2) were employed, where the first takes the input of raw causal parameters, while the second utilizes the variable groups consisting of those normally used in different formulae together with groups of remaining variables in nondimensional forms. This was done to see if the use of the grouped variables produces better results. The Model-A1 thus takes the input in the form of causative factors namely, b, d, f_c', A_s, A_s', f_y, E_s, E_f, b_f, t_f and n and yields the output, which is the IC debonding strain,ε_{fd} of FRP-strengthened RC members

$$\text{Model-A1: } \varepsilon_{fd} = f_1(b, d, f_c', A_s, A_s', f_y, E_s, E_f, b_f, t_f, n) \quad (2)$$

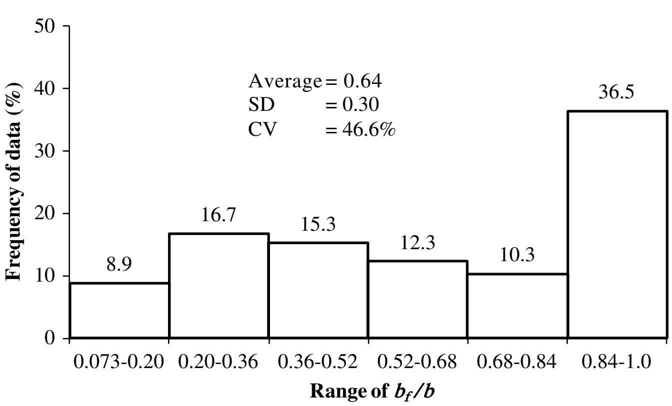

Fig. 1. Frequency distribution of the ratio of width of FRP sheet to the width of concrete section

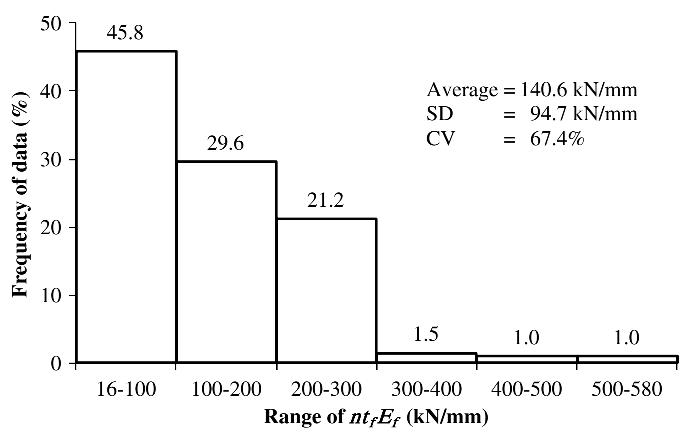

Fig. 3. Frequency distribution of the axial rigidity of FRP sheets

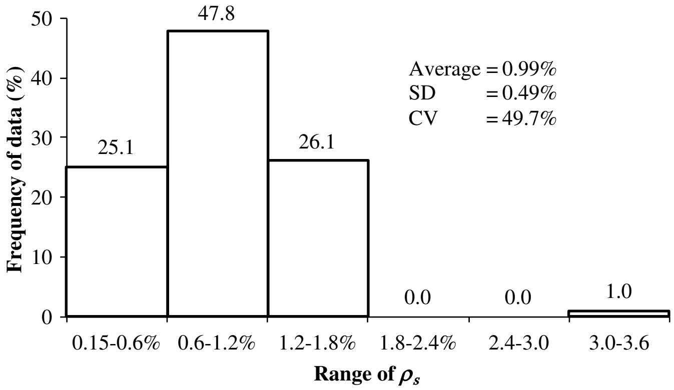

Fig. 4. Frequency distribution of the percentage of tension steel

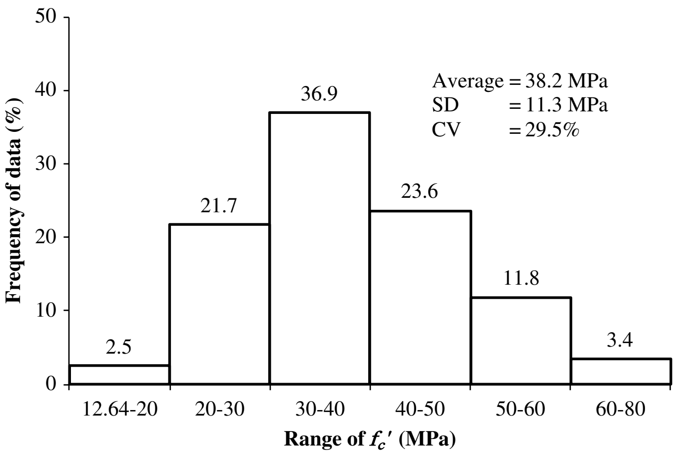

Fig. 5. Frequency distribution of the compressive strength of concrete

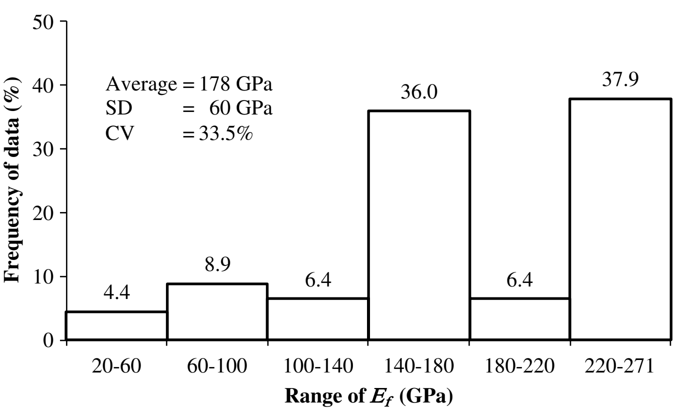

Fig. 6. Frequency distribution of the modulus of elasticity of FRP sheets

Model-A2 employing the grouped variables is given by

$$\text{Model-A2}\ \varepsilon_{fd} = f_2\left(\frac{b_f}{b}, \varepsilon_{sy}, nt_f E_f, \rho_s, \rho_s', f_c'\right) \tag{3}$$

The network architecture of Model-A1 and Model-A2 with one hidden layer employed for the prediction of IC debonding strain of FRP-strengthened RC members, represented by Eqs. (2) and (3),

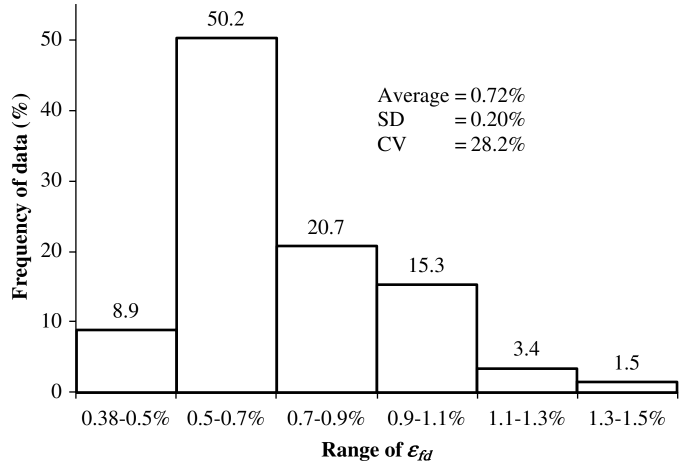

Fig. 7. Frequency distribution of IC debonding strain of FRP sheets

are shown in Figs. 8 and 9, respectively. Another model, namely Model-A3, employing grouped variables but with two hidden layers was also considered (Fig. 10). More hidden layers were avoided because the use of additional hidden layers could make the network too complex.

Three neuron models namely, tansig, logsig and purelin, have been used in the architecture of the network with the back propagation (BP) algorithm. In the back propagation algorithm, the feed-forward (FFBP), cascade-forward (CFBP) and Elman back propagation (EBP) type networks were considered. Each input was weighted with an appropriate weight, and the sum of the weighted inputs and the bias form the input to the transfer function. The neurons employed use of the following differentiable transfer functions to generate their output:

Log-sigmoid transfer function (logsig)

$$y_j = f \cdot \left(\sum_i W_{ij} x_i + \phi_j\right) = \frac{1}{1 + e^{-\left(\sum_i W_{ij} x_i + \phi_j\right)}} \tag{4}$$

Tan-sigmoid transfer function (tansig)

$$y_j = f \cdot \left(\sum_i W_{ij} x_i + \phi_j\right) = \frac{2}{1 + e^{-2\left(\sum_i W_{ij} x_i + \phi_j\right)}} - 1 \tag{5}$$

Linear transfer function (purelin)

$$y_j = f \cdot \left(\sum_i W_{ij} x_i + \phi_j\right) = \sum_i W_{ij} x_i + \phi_j \tag{6}$$

The weight, W, and biases, ϕ, of these equations are determined in such a way as to minimize the energy function. The above transfer functions use the input x to generate layer output y. The suffix i is used for the neurons of a layer, whereas, suffix j is used for the layer number. The number of layers for models with one hidden layer (Figs. 8 and 9) are three, thus requiring two transfer functions, whereas, the number of layers for the model with two hidden layers (Fig. 10) are four thus requiring three transfer functions. The neurons of first hidden layer are generated using the input layer as the input, whereas the generation of the output layer neuron employs the preceding hidden layer as the input. The generation of neurons of second hidden layer employs first hidden layer as the input. The sigmoid transfer functions generate output between 0 and 1 or -1 and $+1$ as the neuron's net input goes from negative to positive

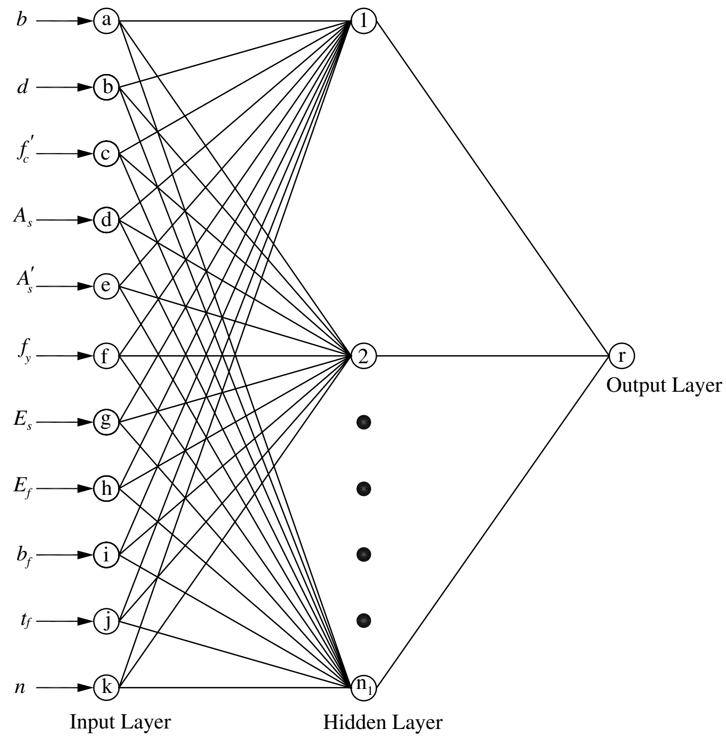

b = width of concrete section
d = effective section depth
f_c' = specified compressive strength of concrete
A_s = area of tension steel
A_s' = area of compression steel
f_y = yield strength of steel
E_s = modulus of elasticity of steel
E_f = tensile modulus of elasticity of FRP material
b_f = width of FRP sheet
t_f = thickness of one ply of FRP reinforcement
n = number of plies of FRP reinforcement

Fig. 8. Model-A1 involving the use of raw variables with one hidden layer ($n_1 = 12$)

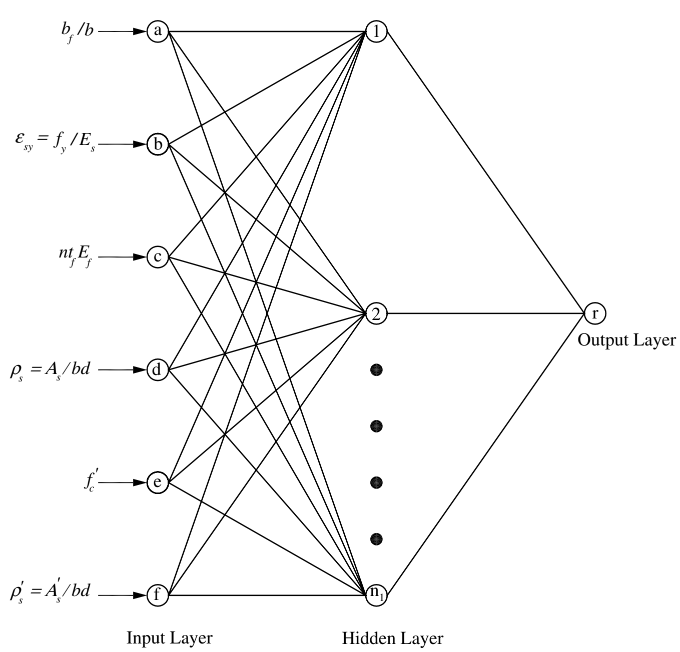

Fig. 9. Model-A2 involving the use of grouped variables with one hidden layer ($n_1 = 12$)

infinity depending upon the use of log or tan sigmoid. When the last layer of a multilayer network has sigmoid neurons (log or tan) then the output of the network is limited to a small range, whereas, the output of linear output neurons can take on any value. The linear output neurons were used for the last layer in the present study because of the wide range of output. Several trials were made for other layers using different combinations of transfer functions and the optimal for single hidden layer was *tansig*, whereas for the two hidden layers these were tansig and *logsig*.

There are three phases involved in ANN modeling, viz. training, validation and testing for which a separate data set is used. The current study used the data described above for the prediction of IC debonding strain (203 data points) of FRP-strengthened RC members. The training of the above two models was done using 67% of the data (136 data points) selected randomly after random sort using a *Matlab* function, *randperm*. Validation and testing of the models was made with the help of the remaining 33% of observations (67 data points), which were not involved in the derivation of the model (Abbas et al. 2011). The training phase is used to adjust the weights on the neural network for which Levenberg-Marquardt nonlinear least square fitting method was employed, whereas, the validation phase is used to minimize over-fitting. In the validation phase, there is no adjustment of the weights of the network with its data set; it is just to verify whether there is any increase in accuracy when a data set that has not been shown

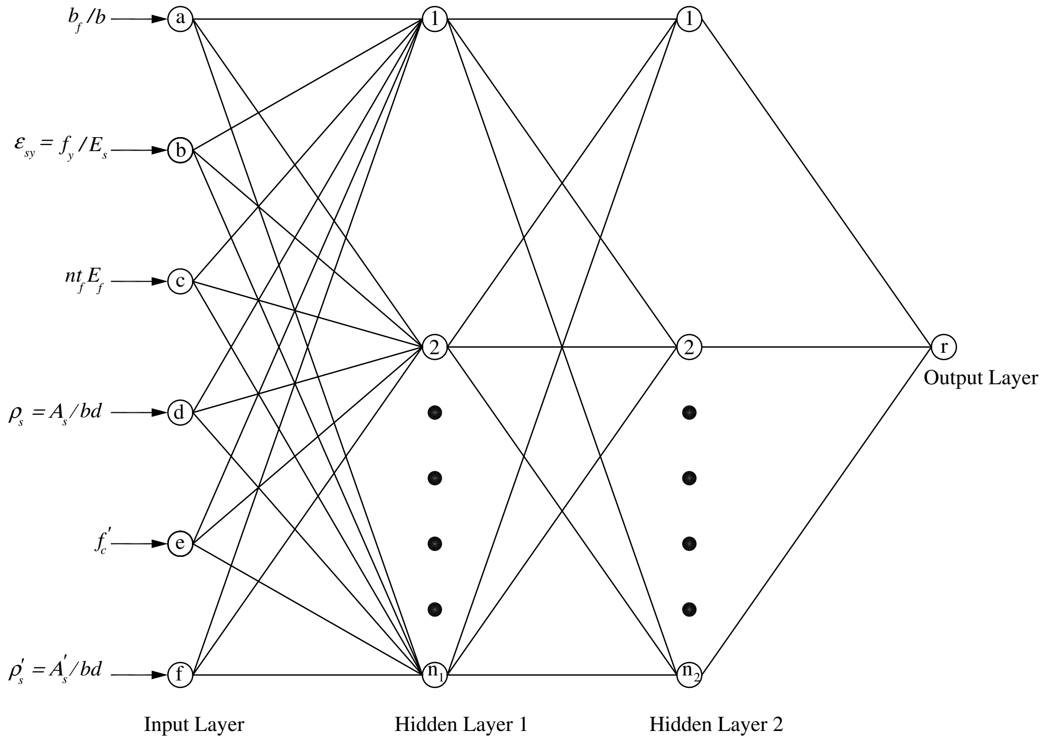

Fig. 10. Model-A3 involving use of grouped variables with two hidden layers ($n_1 = n_2 = 12$)

to the network before (i.e., validation data set) is also added to the training data set. The testing phase is for testing the final solution to confirm the actual predictive power of the network for which different error estimates have been used viz. mean percent error (MPE), mean absolute deviation percent (MAD), root mean square error (RMSE) and correlation coefficient (CC). The parameter MPE gives an idea about the overall characteristic of prediction whether over or under-predicted – positive value indicates over-estimation, whereas, negative value indicates under-estimation.

The optimal architecture was determined by varying the number of hidden neurons. The optimal configuration was based upon minimizing the difference between the neural network predicted value and the desired output. In general, as the number of neurons in the layer is increased, the prediction capability of the network increases in the beginning and then becomes stationary.

The training of the neural network models was stopped when either the acceptable level of error was achieved or when the number of iterations exceeded a prescribed maximum. The neural network model configuration that minimized the MAD and RMSE and optimized the CC was selected as the optimum and the whole analysis was repeated several times.

The preprocessing of the network training set was performed by normalizing the inputs and targets so that their mean is zero and standard deviations as unity. Similarly, all weights and bias values were initialized to random numbers. Although the numbers of input and output nodes are fixed, the hidden nodes in the case of FFBP were subjected to trials, and the one producing the most accurate results (in terms of the RMSE) was selected.

Sensitivity Analysis

Sensitivity tests were conducted to determine the relative significance of each of the independent parameters (input neurons) on the IC debonding strain of FRP-strengthened RC members (output) in both of the models given by Eqs. (2) and (3). In the sensitivity analysis, each input neuron was in turn eliminated from the model and its influence on the prediction of IC debonding strain of FRP-strengthened RC members was evaluated in terms of the MPE, MAD, RMSE and CC criteria. The network architecture of the problem considered in the present sensitivity analysis consists of one or two hidden layers, depending on the model, with 12 neurons decided based on the several iterations. The value of epochs was taken as 100.

The results in Table 6 show that for the prediction of IC debonding strain using Model-A1, the variables in the order of decreasing level of sensitivity are: E_f, n, f_y, b_f, t_f, A_s, b, f_c', d, E_s and A_s'.

Table 6. Sensitivity Analysis of Model-A1 with Feed-Forward Back Propagation for Different Sets of Input Variables

Input variables	MPE	MAD	RMSE	CC
All [Eq. (2)]	1.78	9.73	1,058.9	0.86
No b	3.56	11.40	1,094.0	0.84
No d	1.87	10.51	1,052.0	0.86
No f_c'	1.57	10.57	1,094.6	0.85
No A_s	1.36	11.15	1,118.6	0.84
No A_s'	0.58	10.03	1,056.1	0.86
No f_y	1.39	11.73	1,136.2	0.83
No E_s	1.75	10.65	1,052.4	0.86
No E_f	3.39	13.18	1,326.9	0.77
No b_f	2.12	10.28	1,108.6	0.84
No t_f	1.70	10.62	1,109.7	0.84
No n	1.82	12.11	1,249.6	0.80

Note: CC = correlation coefficient (= R); MAD = mean absolute deviation percent; MPE = mean percent error; RMSE = root mean square error; R^2 = coefficient of determination.

The elimination of the most significant variable E_f is found to have the most significant effect as it reduces the value of CC from 0.86 to 0.77. Most of the available regression models (Tables 1 and 2) for the prediction of IC debonding strain do not include f_y, A_s, A_s', d and E_s. Though A_s', d and E_s do not have significant influence on the IC debonding strain, but the remaining two parameters, f_y and A_s, are the third and sixth most significant parameters whose elimination results in large reduction in the value of CC, thus signifying the importance of their inclusion in the prediction of IC debonding strain of FRP-strengthened concrete.

Table 7 gives the results of sensitivity analysis for Model-A2 of grouped variables. The variables in the order of decreasing level of sensitivity are: nt_fE_f, ε_{sy}, b_f/b, ρ_s, f_c' and ρ_s'. Most of the available models reported in Tables 1 and 2 involve only three grouped variables, nt_fE_f, b_f/b and f_c' thus ignoring the remaining three grouped variables. The reduction in the value of CC from 0.85 to 0.79 for this case indicates that the available models incorporating only limited number of the parameters are not good enough for achieving the desired accuracy and reliability in the estimation of IC debonding strain of FRP-strengthened RC members. These findings are consistent with existing understanding of the relative importance of the various parameters on the IC debonding strain of FRP-strengthened RC members. Further, the elimination of b_f/b besides those eliminated above for other models (i.e., ε_{sy}, ρ_s and ρ_s'), not considered in the ACI-440.2R (2008), JSCE (2001) and Said and Wu (2008) models, reduces the CC to a very low value of 0.74. It is observed from Table 7 that the term ρ_s' has almost no effect on the IC debonding strain; therefore, this has been eliminated in subsequent ANN modeling and in the development of a regression-based model presented later. Model-A2, after eliminating ρ_s', is namdded as Model-A4. The network architecture of Model-A2, after eliminating ρ_s', may thus be used for Model-A4. The IC debonding strain has been taken as microstrain in ANN analysis.

The parameters nt_fE_f and f_c' are given equal weight in ACI-440.2R (2008), Lu et al. (2007) and China Association for Engineering Construction Standardization (CECS 146) (2003) models, whereas the sensitivity analysis indicates that the variables have significantly different levels of sensitivity. For comparing the sensitivity of nt_fE_f and $\sqrt{f_c'}$, which are considered together in many models (Teng et al. 2003; Concrete Society 2004), the analysis was also done by replacing f_c' by $\sqrt{f_c'}$. A comparison of the results of this analysis with that of eliminating f_c' indicates that the levels of sensitivity of nt_fE_f and $\sqrt{f_c'}$ are very much different. It is because of this reason that nt_fE_f and f_c' or $\sqrt{f_c'}$ have not been combined in the present study, and the same approach has also been adopted in the development of a regression-based model presented later.

The results of Model-A3 are also presented in Table 7. The influence of eliminating ρ_s' is also studied for Model-A3, and it is found to have almost no effect. Therefore, the elimination of ρ_s' from the modeling is justified. It is observed from the table that the consideration of two hidden layers in the model does not significantly improve the prediction, and, therefore, sensitivity study was not performed for this model.

Both models (Model-A1 and Model-A2) are almost equally good for the prediction of IC debonding strain (Tables 6 and 7), and the elimination of ρ_s' has almost no influence. Therefore, Model-A4, involving five grouped variables, is recommended because of the use of grouped variables, some of which are also used in the available models.

All the ANN models featured small RMSE during training; however, the value was slightly higher during validation. The models showed consistently good correlation throughout the training and testing. The training and validation for Model-A4 is shown in Fig. 11, whereas training and validation figures for other models being similar have not been included herein. The trained values of connecting weights and bias for Model-A4 for the prediction of IC debonding strain obtained from FFBP training scheme are given in Table 8. The transfer function used between input layer and the hidden layer is Tan-sigmoid as given by Eq. (5), whereas that used between the hidden layer and the output layer is linear given by Eq. (6). The percentage error in the prediction of IC debonding strain by Model-A4 for individual data points is plotted in Fig. 12.

Table 7. Sensitivity Analysis of Model-A2 and Model-A3 with Feed-Forward Back Propagation

Input variables	MPE	MAD	RMSE	CC
Model-A2				
All [Eq. (3)]	2.24	11.86	1,150.6	0.85
No b_f/b	2.09	12.15	1,232.1	0.80
No ε_{sy}	3.19	12.55	1,269.5	0.82
No nt_fE_f	3.82	15.54	1,649.0	0.63
No ρ_s	2.50	12.88	1,221.4	0.80
No ρ_s' (Model-A4)	**−1.50**	**11.62**	**1,124.5**	**0.85**
No f_c'	2.13	11.43	1,160.8	0.84
No b_f/b, ε_{sy}, ρ_s, ρ_s' (ACI 440, JSCE, Said and Wu models)	3.34	13.96	1,374.0	0.74
No ε_{sy}, ρ_s, ρ_s' (Other models)	2.52	12.83	1,251.8	0.79
All [Eq. (3)] but f_c' replaced by $\sqrt{f_c'}$	3.16	11.61	1,182.16	0.84
Model-A3				
All [Eq. (3)]	2.04	11.01	1,103.6	0.85
No ρ_s'	2.72	11.09	1,124.8	0.85

Note: MPE = mean percent error; MAD = mean absolute deviation percent; RMSE = root mean square error; CC = correlation coefficient (= R); R^2 = coefficient of determination; the model in bold is the one recommended for adoption.

Regression Model

A new regression model for the prediction of IC debonding strain of FRP-strengthened RC members is developed by employing

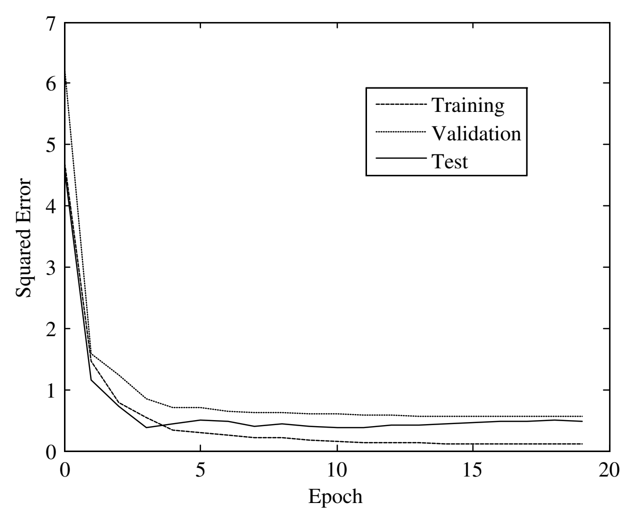

Fig. 11. Epochs versus squared error for prediction of IC debonding strain by back propagation using Model-A4

Table 8. Connection Weights and Biases for Model-A2 Used for the Prediction of IC Debonding Strain (Refer to Fig. 9) (Transfer Functions: *Tansig and Purelin*; Output Layer Bias, $\phi_2 = 1.6558$ and $R^2 = 0.71$)

Neuron	Input-Hidden layer weights, W_1					Hidden layer-output weight, W_2	Hidden layer bias, ϕ_1
	f'_c	ρ_s	ε_{sy}	b_f/b_c	nt_fE_f		
1	0.0648	−1.4206	−0.6012	1.0570	0.8304	1.3288	−3.1454
2	0.4096	0.3751	1.2147	−0.9596	−0.4178	0.6069	−1.5398
3	0.1388	−1.3899	1.1750	−1.8351	3.0881	−1.1060	−0.2786
4	−1.0833	−1.8121	1.2491	0.8115	−0.2048	1.2108	−1.9681
5	−1.2646	0.0085	−0.9504	2.7265	−1.2331	1.3869	0.4460
6	2.2057	−0.5980	1.1421	−1.6243	−0.2525	0.9939	0.6020
7	1.1136	−0.7679	0.4671	−0.5395	1.0212	−1.1955	1.3452
8	0.3633	−0.4882	0.8014	−1.1456	2.0594	2.4125	−0.0144
9	0.3102	−0.0256	−0.0523	0.3312	−0.6911	−1.9779	−0.9526
10	0.2266	0.6331	−0.6085	1.3809	−1.9198	−1.2732	2.2704
11	−0.8104	−0.8977	1.3896	−1.3438	1.3736	−1.1095	2.4341
12	−0.8424	−0.3937	−0.4099	0.8635	1.4561	−1.2035	−3.1696

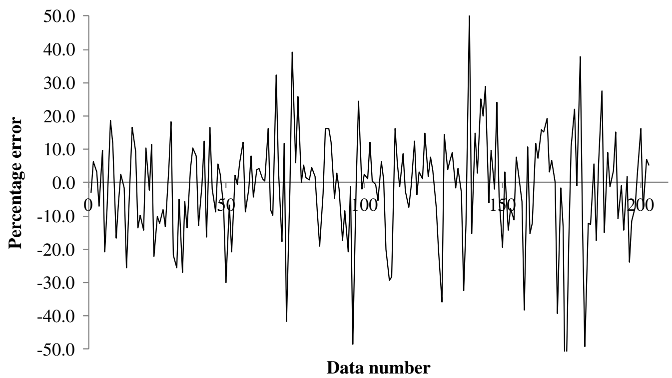

Fig. 12. Percentage error in prediction of IC debonding strain using Model-A4 for individual data points

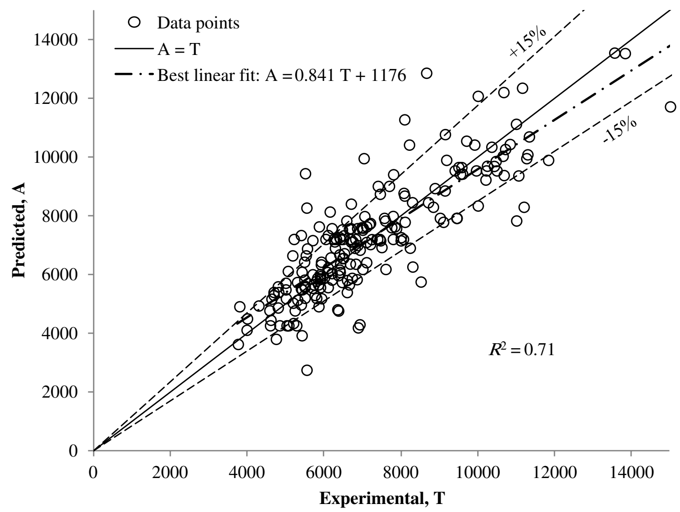

Fig. 13. Observed versus predicted IC debonding strain of FRP-strengthened RC members for Model-A4

the grouped variables found sensitive from the sensitivity analysis presented above for ANN models. The best fit regression model is

$$\varepsilon_{fd} = \left(\frac{2 - b_f/b}{1 + b_f/b}\right)^{0.1} \left(\frac{\varepsilon_{sy}}{nt_fE_f}\right)^{0.4} \left(6.5 + \frac{nt_fE_f}{135{,}000}\right) \rho_s^{0.05} f_c'^{0.1} \tag{7}$$

The above model further confirms the observation made in the sensitivity analysis presented above for ANN models that nt_fE_f and f'_c or $\sqrt{f'_c}$ have different levels of sensitivity thus considering them together, as done in most of the models, is not justified. The low power of f'_c appearing in the above equation indicates that the IC debonding strain is proportional to the square root of the fracture energy, $G_f[G_f = k(f'_c)^{0.2}]$ which is considered by the JSCE (2001) model. The above model also shows that nt_fE_f is the most significant parameter as observed earlier in the sensitivity analysis. The variable ε_{sy}, which was found to be the second most significant variable from the sensitivity analysis presented above, is also confirmed to have significant influence on the prediction of IC debonding strain.

The predicted value of the IC debonding strain has been plotted against its observed value in Figs. 13 and 14 for Model-A4 and the best fit regression model, respectively. The histograms of error in the prediction using Model-A4 and the proposed regression model are plotted in Fig. 15. Though the best linear fit line between the

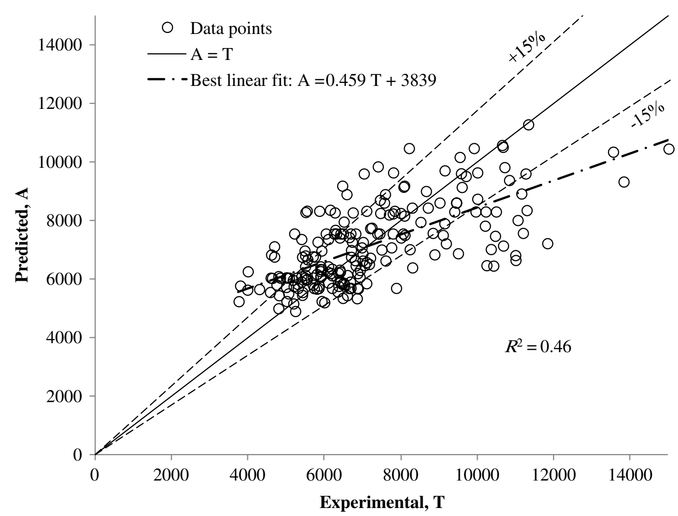

Fig. 14. Observed versus predicted IC debonding strain for regression model of Eq. (7)

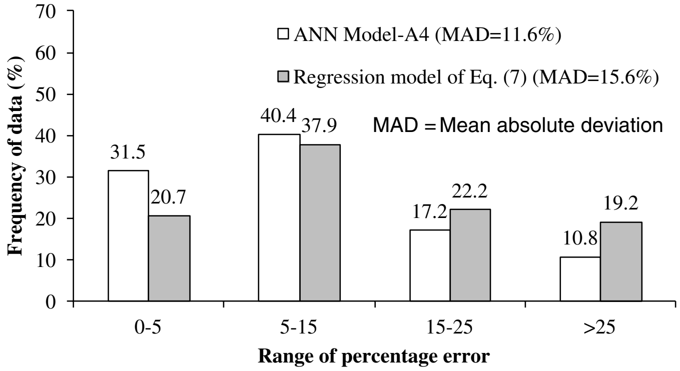

Fig. 15. Histogram of percentage error for different models of IC debonding strain

Table 9. Error Estimates for Different Models

	IC debonding strain	
Parameter for error estimate	ANN Model-A4	Regression model of Eq. (7)
Mean percent error (MPE)	−1.50	−3.17
Mean absolute deviation in percent (MAD)	11.62	15.6
Root mean square error (RMSE)	1,124.5	1,496.2
Coefficient of correlation (CC)	0.85	0.67
Percent data for error within 15%	71.9	58.6
Percentage error enveloping 80% data	17.3	24.8

experimental and the predicted values is very close to the line of goodness of fit (i.e., experimental = predicted line) for ANN Model-A4 (Fig. 13), but for the regression model the two lines are not close (Fig. 14). This shows that the regression model slightly underestimates the IC debonding strain for higher strain values which also proves the superiority of the proposed ANN model to the regression model. The error estimates for the best fit ANN model (Model-A4) and best fit regression model for IC debonding strain are summarized in Table 9. Besides the four error estimates considered above for the ANN models, two additional estimates (viz. percent data for error within 15% range and percentage of error enveloping 80% of the data) for judging the performance of models are also given in Table 9.

The mean error in the proposed regression model is 15.6%; whereas, the mean error in neural network Model-A4 is only 11.6%. A comparison of ANN Model-A4 with the proposed regression model shows that more than 71.9% of the data have error less than 15% for Model-A4 whereas, only 58.6% of the data have the same percentage of error for the regression model (Fig. 15). It is also observed from Table 9 that for about 80% of the data, the percentage error is less than 17.3% for the ANN Model-A4, whereas the percentage error in the regression-based model for the same percentage of data is about 24.8%. This indicates that the neural network model is better fitting the experiments than the regression best fit model. ANN Model-A4 also shows higher CC $(= 0.85)$, lower MPE $(= -1.50)$ and lover RMSE $(= 1{,}124.5)$.

Proposed Design Models and Comparison with Existing Models

The best fit regression model of Eq. (7) is converted to the design model by considering a reduction factor of 1.55. The value of the reduction factor was decided such that there is a minimum factor of safety of 1.1 for 95% data. The proposed design model is thus given by

$$\varepsilon_{fd} = \frac{1}{1.55}\left(\frac{2 - b_f/b}{1 + b_f/b}\right)^{0.1}\left(\frac{\varepsilon_{sy}}{nt_f E_f}\right)^{0.4}\left(6.5 + \frac{nt_f E_f}{135{,}000}\right)\rho_s^{0.05} f_c'^{0.1} \tag{8}$$

For all data points, the distance from the FRP end to the section of maximum moment (L_d) was found to be greater than the effective bond length given by $L_e = \sqrt{nE_f t_f/\sqrt{f_c'}}$ and hence, the factor k_L proposed by Teng et al. (2003), as given in Table 2, was estimated to be 1.0 for all experimental data. Accordingly, the factor k_L was omitted from our proposed model.

A reduction factor for the ANN model was also calculated for keeping a minimum factor of safety of 1.1 for 95% of the data, as considered above, and its value was obtained as 1.41. Introducing this reduction factor in the best fit network configuration (FFBP Model-A4) with the transfer functions of Tan-sigmoid and linear, some of the weight and bias values given in Table 8 get modified. The modified values are: output layer bias, $\phi_2 = 1.1743$ and the output layer weight, W_2 given by:

$$W_2 = [0.9424 \quad 0.4304 \quad -0.7844 \quad 0.8587 \quad 0.9836 \quad 0.7049 \quad -0.8479 \quad 1.7110 \quad -1.4028 \quad -0.9030 \quad -0.7869 \quad -0.8535]$$

and all other weights and biases remain the same as given in Table 8.

For the sake of comparison of the proposed design models with the available models, the predicted IC debonding strain is compared with the experimental values. IC debonding strain predicted by codal equations and different researchers are plotted in Figs. 16 and 17, respectively, whereas those predicted by the proposed design models are plotted in Fig. 18. For getting an idea about the scatter in the predictions, percentile plots for deviation in the predictions by all the models are plotted in Fig. 19. The height of bars varies from the lower to the upper limit of deviation. Four quartiles of deviation from experiment are shown in the figure. Ideally, the vertical bar should be almost above the zero line, should have minimum height and the height of 2nd and 3rd quartiles should be minimum.

The ratio of experimental to the predicted value of IC debonding strain was also evaluated for the purpose of assessment of various models. Some statistical parameters viz. mean, standard deviation, coefficient of variation and 5th percentile, evaluated for different models are listed in Table 10. Percentage of nonconservative data

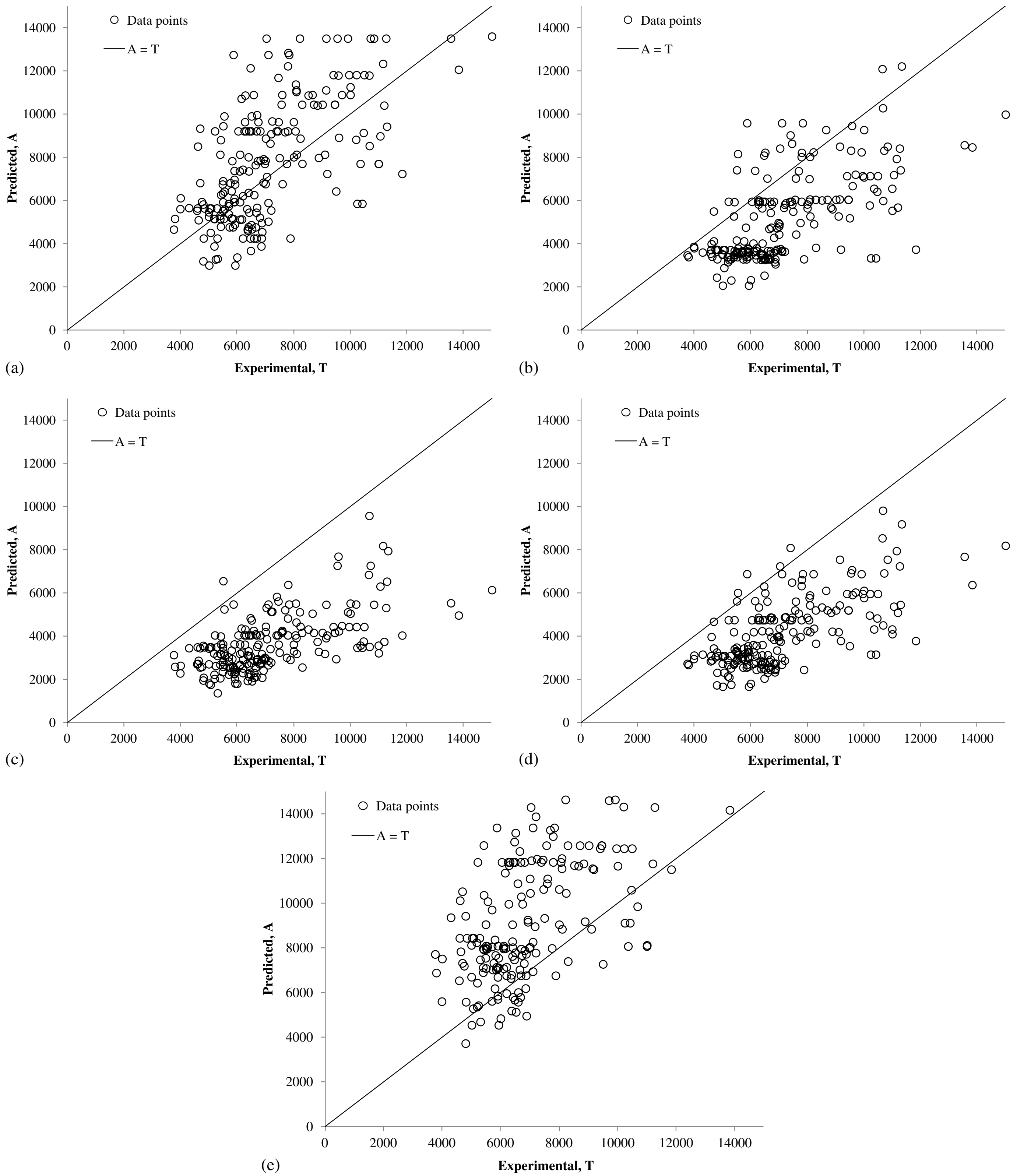

Fig. 16. Comparison of IC debonding strain predicted by models of different codes with the experiment: (a) ACI 440.2R (2008) design version; (b) JSCE (2001) design version; (c) Concrete society (2004) design version; (d) Italian code (NRC 2012) design version; (e) Chinese code (2003) design version

is also given in the table for each model. Ideally, standard deviation and coefficient of variation should be low, 5th percentile should be close to 1.1, mean should be greater than 1 but not very large and the nonconservative data points should be close to zero.

Among five models of different codes considered in the study, all are nonconservative except for Concrete Society model (2004) where the nonconservative data is only 0.5%. ACI 440.2R (2008) and Chinese code (2003) models are the most nonconservative.

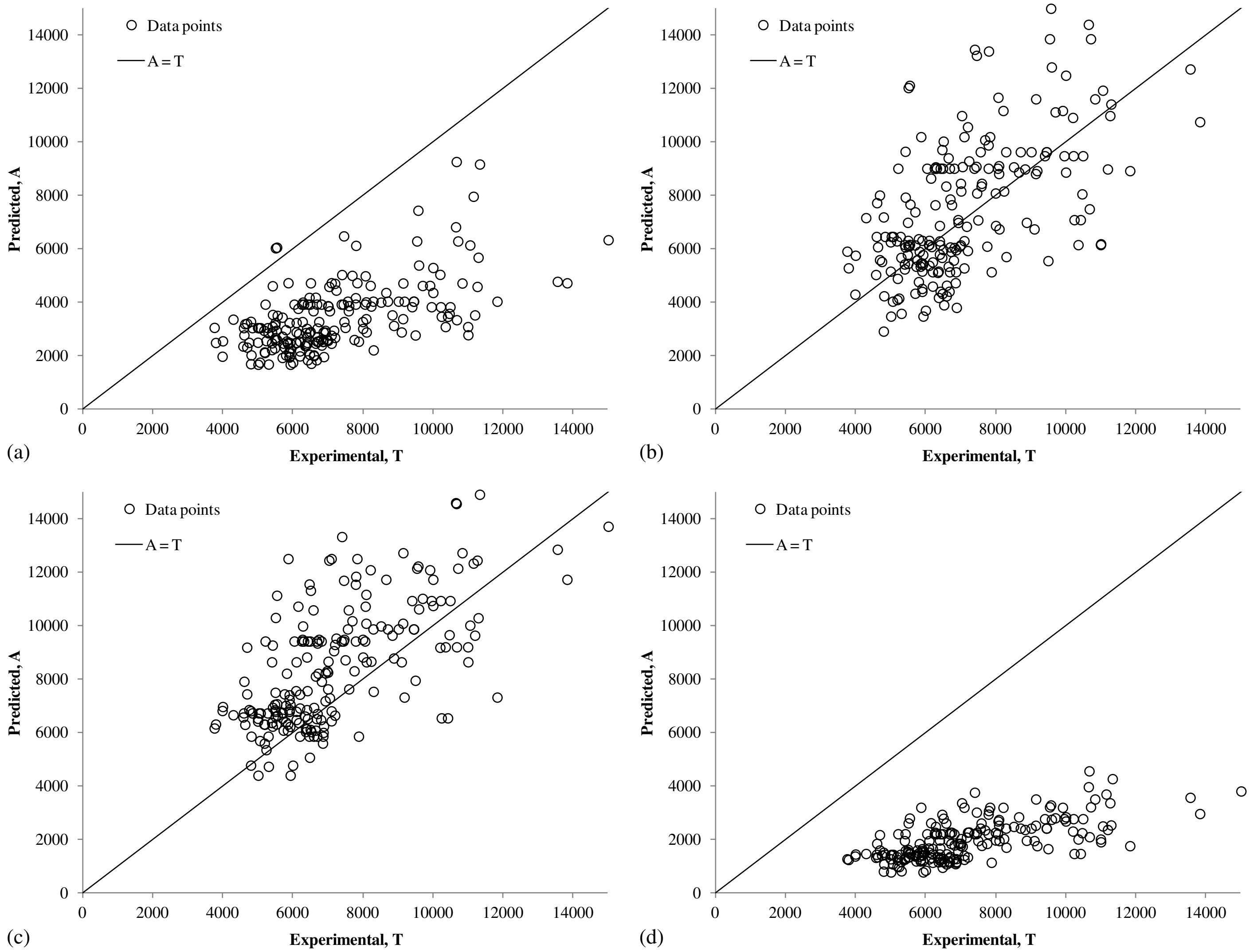

Fig. 17. Comparison of IC debonding strain predicted by models of different researchers with experiment: (a) Teng et al. (2003); (b) Lu et al. (2007); (c) Said and Wu (2008); (d) Bilotta et al. (2013)

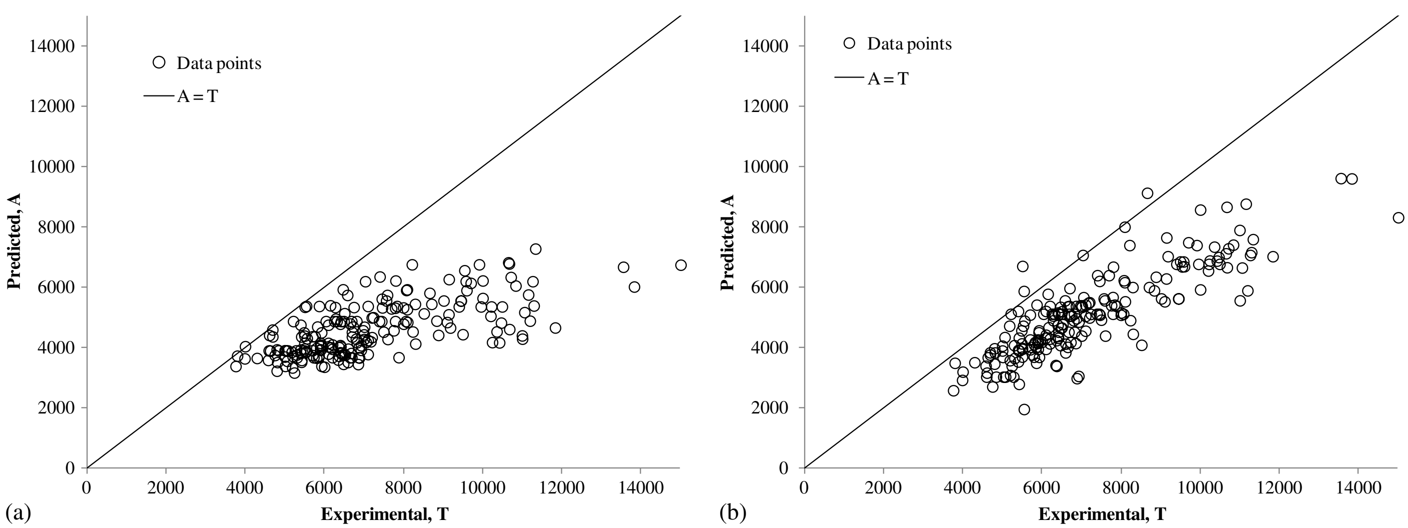

Fig. 18. Comparison of IC debonding strain predicted by proposed design models with experiment: (a) Regression model of Eq. (8); (b) ANN Model-A4

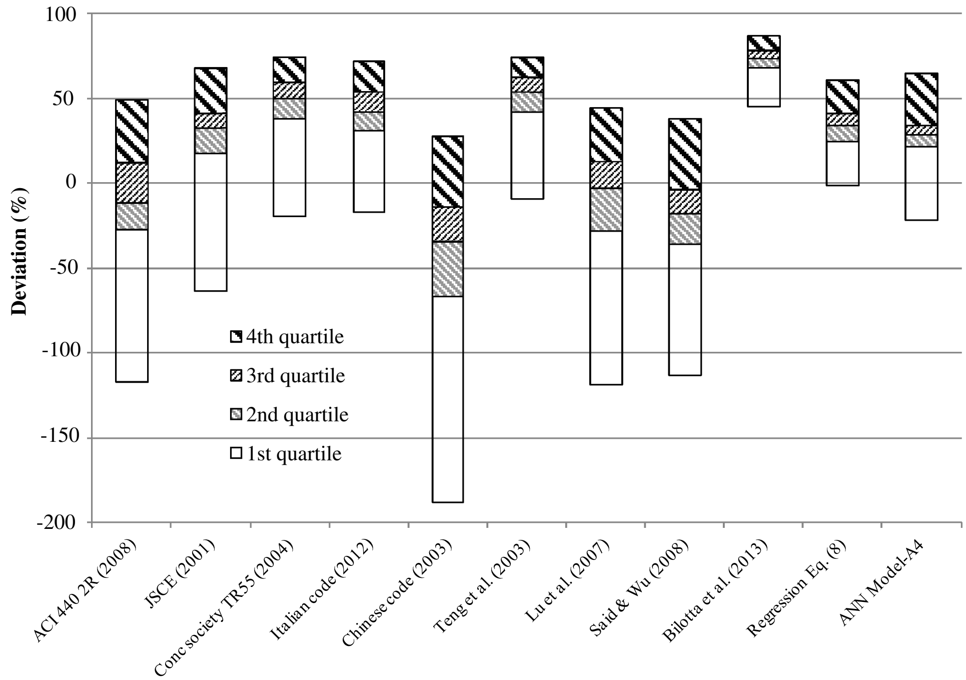

Fig. 19. Spread of percentile for different models

Table 10. Statistical Parameters for the Assessment of Models (203 data points)

Model	Statistical parameters for experimental to predicted ratio				Non-conservative data (%)
	Mean	SD	CV (%)	5th percentile value	
ACI 440.2R (2008)	0.98	0.31	24.19	0.58	62.6
JSCE (2001)	1.50	0.44	32.44	0.85	10.3
Concrete Society (2004)	2.08	0.58	47.55	1.30	0.5
Italian code (NRC 2012)	1.84	0.54	42.21	1.09	2.5
Chinese code (2003)	0.77	0.22	17.58	0.45	84.7
Teng et al. (2003)	2.23	0.62	51.34	1.29	1.0
Lu et al. (2007)	1.00	0.29	22.98	0.59	57.1
Said and Wu (2008)	0.87	0.20	15.34	0.57	76.8
Bilotta et al. (2013)	3.95	1.16	90.89	2.35	0.0
Regression model of Eq. (8)	1.56	0.32	24.12	1.10	0.5
ANN Model-A4	1.42	0.24	16.61	1.10	2.0

Note: CV = coefficient of variation; SD = standard deviation.

Among four researchers' models, Lu et al. (2007) and Said and Wu (2008) models are nonconservative, whereas Bilotta et al. model (2013) is most conservative with the vertical bar lying far above the zero deviation line (Fig. 19). Teng et al. (2003) model is the best among all the available models, but the model has large scatter (SD = 0.62 and CV = 51.34% for the experiment to predicted ratio), and the model is conservative owing to its high mean of experimental to predicted ratio (= 2.23). The proposed design models, namely ANN Model-A4 and regression model of Eq. (8), are however the best among all the available models showing balanced values of all the above parameters used for the assessment of various models. It is worth mentioning here that the value of 5th percentile for the proposed design models is 1.1 because this was the target for deciding reduction factors in the proposed design equations.

Conclusions

A model for predicting the IC debonding strain of FRP-strengthened RC members using neural network has been developed. The network predictions were generally more satisfactory than those given by traditional regression equations and the one developed in this study because of low errors and high correlation coefficients. The IC debonding strain predictions based on raw data were almost the same as those based on the grouped variables and thus the grouped variables are recommended for adoption because of its simplicity and the use of some of these groups in available models. The neural network with one hidden layer was selected as the optimum network to predict the IC debonding strain. Thus, network configuration of Model-A4 with FFBP is recommended for general use o predict the IC debonding strain of FRP-strengthened RC members. On the basis of sensitivity analysis for the prediction of IC debonding strain, it is observed that the axial rigidity of the FRP system ($nt_f E_f$), yields strain of steel rebars, and the ratio of the width of FRP sheet to the width of the rib of the beam/slab are the three most significant parameters for the prediction of IC debonding strain of FRP-strengthened RC members. Some of the significant parameters, missing in available models, have been incorporated in a new regression model proposed in the paper. The neural network model is however better than the regression model in the prediction of the IC debonding strain of FRP-strengthened RC members.

Acknowledgments

The authors would like to extend their sincere appreciation to the *Deanship of Scientific Research* at King Saud University for its funding of this research through the research group project No. RGP-VPP-310. Thanks are also extended to the MMB Chair for Research and Studies in Strengthening and Rehabilitation of Structures, at the Department of Civil Engineering, King Saud University for providing technical support.

References

Abbas, H., Alsayed, S. H., Amusallam, T. H., and Al-Salloum, Y. A. (2011). "Characterization of hole-diameter in thin metallic plates perforated by spherical projectiles using genetic algorithms." *Arch. Appl. Mech.*, 81(7), 907–924.

ACI Committee 318. (2011). "Building code requirements for reinforced concrete and commentary." *ACI 318-11*, Farmington Hills, MI.

ACI Committee 440. (2008). "Guide for the design and construction of externally bonded FRP systems for strengthening concrete structures." *ACI 440.2R-08*, Farmington Hills, MI.

Adhikary, B. B., and Mutsuyoshi, H. (2006). "Prediction of shear strength of steel fiber RC beams using neural networks." *Constr. Build. Mater.*, 20(9), 801–811.

Ai-hui, Z., Wei-liang, J., and Gui-bing, L. (2006). "Behavior of preloaded RC beams strengthened with CFRP laminates." *J. Zhejiang Univ. SCI. A*, 7(3), 436–444.

Alagusundaramoorthy, P., Harik, I. E., and Choo, C. C. (2002). "Flexural behavior for R/C beams strengthened with CFRP sheets or fabric." *Research Rep. KTC-02-13/SPR 200-99-1F*, Kentucky Transportation Center, College of Engineering, Univ. of Kentucky, Lexington, KY.

Al-Negheimish, A. I., Shuraim, A. B., Al-Zaid, R. Z., Al-Huzaimy, A. M., and El-Sayed, A. K. (2011). "Innovative procedure for strengthening wide shallow beam floor system using CFRP reinforcement." *2nd year progress Rep., submitted to center of excellence for research in engineering materials (CEREM)*, King Saud Univ., Riyadh, Saudi Arabia.

Al-Rousan, R., Issa, M., and Shabila, H. (2012). "Performance of reinforced concrete slabs strengthened with different types and configurations of CFRP." *Compos. B Eng.*, 43(2), 510–521.

Al-Zaid, R. Z., Shuraim, A. B., El-Sayed, A. K., Al-Negheimish, A. I., and Al-Huzaimy, A. M. (2010). "Flexural strengthening of shallow reinforced concrete beams using CFRP plates." *2nd Int. Structural Specialty Conf. (on CD-R)*, CSCE, Winnipeg, Canada.

Arduini, M., Di Tommaso, A., and Nanni, A. (1997). "Brittle failure in FRP plate and sheet bonded beams." *ACI Struct. J.*, 94(4), 363–370.

Arduini, M., and Nanni, A. (1997). "Behavior of precracked RC beams strengthened with carbon FRP sheets." *J. Compos. Constr.*, 10.1061/(ASCE)1090-0268(1997)1:2(63), 63–70.

Azevedo, D. M. M., Juvandes, L. F. P., and Henriques, A. A. R. (2005). "Flexural strengthening with FRP systems experimental results vs. expected results based on actual design guidelines." *3rd Int. Conf. on Composites in Construction*, Lyon, France.

Bakay, R., Sayed-Ahmed, E. Y., and Shrive, N. G. (2009). "Interfacial debonding failure for reinforced concrete beams strengthened with carbon-fibre-reinforced polymer strips." *Can. J. Civ. Eng.*, 36(1), 103–121.

Bakis, C. E., et al. (2002). "Fiber-reinforced polymer composites for construction – State-of-the-art review." *J. Compos. Constr.*, 10.1061/(ASCE)1090-0268(2002)6:2(73), 73–87.

Bilotta, A., Faella, C., Martinelli, E., and Nigro, E. (2013). "Design by testing procedure for intermediate debonding in EBR FRP strengthened RC beams." *Eng. Struct.*, 46, 147–154.

Bonacci, J. F., and Maalej, M. (2000). "Externally bonded fiber-reinforced polymer for rehabilitation of corrosion damaged concrete beams." *ACI Struct. J.*, 97(5), 703–711.

Breña, S. F., Bramblett, R. M., Wood, S. L., and Kreger, M. E. (2003). "Increasing flexural capacity of reinforced concrete beams using carbon fiber-reinforced polymer composites." *ACI Struct. J.*, 100(1), 36–46.

Breña, S. F., and Macri, B. M. (2004). "Effect of carbon-fiber-reinforced polymer laminate configuration on the behavior of strengthened reinforced concrete beams." *J. Compos. Constr.*, 10.1061/(ASCE)1090-0268(2004)8:3(229), 229–240.

Bsisu, K., Hunaiti, Y., and Younes, R. (2012). "Flexural ductility behavior of strengthened reinforced concrete beams using steel and CFRP plates." *Jordan J. Civ. Eng.*, 6(3), 304–312.

Buyukozturk, O., and Hearing, B. (1998). "Failure behavior of precracked concrete beams retrofitted with FRP." *J. Compos. Constr.*, 10.1061/(ASCE)1090-0268(1998)2:3(138), 138–144.

Cameron, R. (2012). "Strengthening of RC beams with externally bonded and anchored FRP laminate." M.S. thesis, McMaster Univ., Hamilton, ON, Canada.

Ceroni, F. (2010). "Experimental performances of RC beams strengthened with FRP materials." *Constr. Build. Mater.*, 24(9), 1547–1559.

Chahrour, A., and Soudki, K. (2005). "Flexural response of reinforced concrete beams strengthened with end-anchored partially bonded carbon fiber-reinforced polymer strips." *J. Compos. Constr.*, 10.1061/(ASCE)1090-0268(2005)9:2(170), 170–177.

China Association for Engineering Construction Standardization (CECS 146). (2003). "Technical specification for strengthening concrete structure with carbon fiber reinforced polymer laminate." China Planning Press, Beijing.

Concrete Society. (2004). "Design guidance for strengthening concrete structures using fibre composite materials." *Concrete Society Technical Rep. 55*, 2nd Ed., Camberley, Surrey, U.K.

David, E., Djelal, C., and Buyle-Bodin, F. (1998). "Repair and strengthening of reinforced concrete beams using composite materials." *2nd Int. Ph.D. Symp. in Civil Engineering*, Structural Concrete Laboratory of EPFL, Lausanne, Switzerland.

Dias, S., Juvandes, L., and Figueiras, J. (2004). "Strengthening of reinforced concrete structures in bending with CFRP." *Revista IBRACON de Estructuras*, 1(1), 1–19.

Elsanadedy, H. M., Al-Salloum, Y. A., Abbas, H., and Alsayed, S. H. (2012). "Prediction of strength parameters of FRP confined concrete." *Compos. B Eng.*, 43(2), 228–239.

Fang, T. Q. (2002). "Study on U-shaped sheet behavior of anti-debonding in the concrete beam reinforced flexurally with FRP." M.S. thesis, Tsingua Univ., China.

Fanning, P. J., and Kelly, O. (2001). "Ultimate response of RC beams strengthened with CFRP plates." *J. Compos. Constr.*, 10.1061/(ASCE)1090-0268(2001)5:2(122), 122–127.

Farah, K., and Sato, Y. (2007). "Numerical simulation of debonding failure of reinforced concrete beams strengthened with externally bonded FRP." *Asia-Pacific Conf. on FRP in Structures (APFIS 2007)*, Dept. of Civil Engineering, Univ. of Hong Kong, Hong Kong, 799–804.

GangaRao, H. V. S., and Vijay, P. V. (1998). "Bending behavior of concrete beams wrapped with carbon fabric." *J. Struct. Eng.*, 10.1061/(ASCE)0733-9445(1998)124:1(3), 3–10.

Gao, D., You, P., and Zhan, C. (2011). "Crack resistant performance and crack width of one-way slabs strengthened with FRP." *Appl. Mech. Mater.*, 71–78, 3810–3815.

Grace, N. F., Abdel-Sayed, G., and Ragheb, W. F. (2002). "Strengthening of concrete beams using innovative ductile fiber-reinforced polymer fabric." *ACI Struct. J.*, 99(5), 692–700.

Grace, N. F., Ragheb, W. F., and Abdel-Sayed, G. (2003). "Flexural and shear strengthening of concrete beams using new triaxially braided ductile fabric." *ACI Struct. J.*, 100(6), 804–814.

Grace, N. F., and Singh, S. B. (2005). "Durability evaluation of carbon fiber-reinforced polymer strengthened concrete beams: Experimental study and design." *ACI Struct. J.*, 102(1), 40–53.

Gunes, O., Buyukozturk, O., and Karaca, E. (2009). "A fracture-based model for FRP debonding in strengthened beams." *Eng. Fract. Mech.*, 76(12), 1897–1909.

Japan Society of Civil Engineers (JSCE). (2001). "Recommendations for upgrading of concrete structures with use of continuous fiber sheets."

Concrete Engineering Series 41, Japan Society of Civil Engineers, Japan, 256.

Juvandes, F. P. L. (1999). "Strengthening and rehabilitation of concrete structures using CFRP composites." Ph.D. dissertation, Faculty of Engineering, Univ. of Porto (FEUP), Portugal (in Portuguese).

Kaminska, M. E., and Kotynia, R. (2000). "Experimental research on RC beams strengthened with CFRP strips." *Rep. No. 9*, Dept. of Concrete Structures, Technical Univ. of Lodz, Poland.

Karbhari, V. M., Niu, H., and Sikorsky, C. (2006). "Review and comparison of fracture mechanics-based bond strength models for FRP-strengthened structures." *J. Reinforc. Plast. Compos.*, 25(17), 1757–1794.

Khomwan, N., Foster, S. J., and Smith, S. T. (2004). "Debonding failure in CFRP strengthened concrete beams." *Proc., 2nd Int. Conf. on FRP Composites in Civil Engineering (CICE 2004)*, Taylor and Francis Group, London.

Kim, Y. J., Green, M. F., and Fallis, G. J. (2008a). "Repair of bridge girder damaged by impact loads with prestrtessed CFRP sheets." *J. Bridge Eng.*, 10.1061/(ASCE)1084-0702(2008)13:1(15), 15–23.

Kim, Y. J., Wight, R. G., and Green, M. F. (2008b). "Flexural strengthening of RC beams with prestressed CFRP sheets: Using non-metallic anchor systems." *J. Compos. Constr.*, 10.1061/(ASCE)1090-0268(2008)12:1(44), 44–52.

Kotynia, R. (2005). "Debonding failures of RC beams strengthened with externally bonded strips." *Proc., Int. Symp. on Bond Behavior of FRP in Structures (BBFS 2005)*, International Institute for FRP in Construction.

Kotynia, R., and Kaminska, M. E. (2003). "Ductility and failure mode of RC beams strengthened for flexure with CFRP." *Rep. No. 13*, Dept. Concrete Structures, Technical Univ. of Lodz, Poland.

Kotynia, R., Walendziak, R., Stoecklin, I., and Meier, U. (2011). "RC slabs strengthened with prestressed and gradually anchored CFRP strips under monotonic and cyclic loading." *J. Compos. Constr.*, 10.1061/(ASCE)CC.1943-5614.0000081, 168–180.

Kurtz, S., and Balaguru, P. (2001). "Comparison of inorganic and organic matrices for strengthening of RC beams with carbon sheets." *J. Struct. Eng.*, 10.1061/(ASCE)0733-9445(2001)127:1(35), 35–42.

Kurtz, S., Balaguru, P., and Helm, J. (2008). "Experimental study of interfacial shear stresses in FRP-strengthened RC beams." *J. Compos. Constr.*, 10.1061/(ASCE)1090-0268(2008)12:3(312), 312–322.

Lee, S., and Moy, S. (2007). "A method for predicting the flexural strength of RC beams strengthened with carbon fiber reinforced polymer." *J. Reinforc. Plast. Compos.*, 26(14), 1383–1401.

Lopez, A., and Nanni, A. (2006). "Composite strengthening technologies." *Concr. Int.*, 28(1), 74–80.

Lu, X. Z., Teng, J. G., Ye, L. P., and Jiang, J. J. (2007). "Intermediate crack debonding in FRP-strengthened RC beams: FE analysis and strength model." *J. Compos. Constr.*, 10.1061/(ASCE)1090-0268(2007)11:2(161), 161–174.

Maalej, M., and Leong, K. S. (2005). "Effect of beam size and FRP thickness on interfacial shear stress concentration and failure mode of FRP-strengthened beams." *Compos. Sci. Technol.*, 65(7–8), 1148–1158.

Matthys, S. (2000). "Structural behavior and design of concrete beams strengthened with externally bonded FRP reinforcement." Ph.D. thesis, Ghent Univ., Gent, Belgium.

Mazzotti, C., Savoia, M., and Ferracuti, B. (2008). "An experimental study on delamination of FRP plates bonded to concrete." *Constr. Build. Mater.*, 22(7), 1409–1421.

Meier, U. (1995). "Strengthening of structures using carbon fibre/epoxy composites." *Constr. Build. Mater.*, 9(6), 341–351.

Napoli, A. (2008). "RC structures strengthened with mechanically fastened FRP systems." M.S. thesis, Univ. of Miami, Florida.

National Research Council (NRC). (2012). "Guide for the design and construction of externally bonded FRP systems for strengthening existing structures (CNR-DT200 R1/2012)." Rome.

Neagoe, C. A. (2011). "Concrete beams reinforced with CFRP laminates." M.S. thesis, Polytechnic Univ. of Catalonia, Spain.

Oehlers, D. J., Park, S. M., and Ali, M. S. M. (2003). "A structural engineering approach to adhesive bonding longitudinal plates to RC beams and slabs." *Compos. Appl. Sci. Manuf.*, 34(9), 887–897.

Pan, J., Leung, C. K. Y., and Luo, M. (2010). "Effect of multiple secondary cracks on FRP debonding from the substrate of reinforced concrete beams." *Constr. Build. Mater.*, 24(12), 2507–2516.

Park, S. Y. (2001). "Ultimate strength of precast high-strength concrete beams strengthened in bending with different steel and glued FRP reinforcement ratios." *KSCE J. Civ. Eng.*, 5(4), 339–345.

Pham, H. B., and Al-Mahaidi, R. (2006). "Prediction models for debonding failure loads of carbon fiber reinforced polymer retrofitted reinforced concrete beams." *J. Compos. Constr.*, 10.1061/(ASCE)1090-0268(2006)10:1(48), 48–59.

Quattlebaum, J., Harries, K. A., and Petrou, M. F. (2005). "Comparison of three CFRP flexural retrofit systems under monotonic and fatigue loads." *J. Bridge Eng.*, 10.1061/(ASCE)1084-0702(2005)10:6(731), 731–740.

Rahimi, H., and Hutchinson, A. (2001). "Concrete beams strengthened with externally bonded FRP plates." *J. Compos. Constr.*, 10.1061/(ASCE)1090-0268(2001)5:1(44), 44–56.

Ramanathan, K. N. (2008). "Influence of FRP width-to-spacing ratio on bond performance of externally bonded FRP systems on one way concrete slabs." M.S. thesis, Univ. of Pittsburgh, Pittsburgh, PA.

Reeve, B. Z. (2005). "Effect of adhesive stiffness and CFRP geometry on the behavior of externally bonded CFRP retrofit measures subject to monotonic loads." M.S. thesis, Univ. of Pittsburgh, Pittsburgh, PA.

Rusinowski, P., and Täljsten, B. (2009). "Intermediate crack induced debonding in concrete beams strengthened with CFRP plates – An experimental study." *Adv. Struct. Eng.*, 12(6), 793–806.

Saadatmanesh, H., and Ehsani, M. R. (1991). "RC beams strengthened with GFRP plates. I: Experimental study." *J. Struct. Eng.*, 10.1061/(ASCE)0733-9445(1991)117:11(3417), 3417–3433.

Said, H., and Wu, Z. (2008). "Evaluating and proposing models of predicting IC debonding failure." *J. Compos. Constr.*, 10.1061/(ASCE)1090-0268(2008)12:3(284), 284–299.

Salib, M. N. (2012). "Flexural behavior of RC T- section beams strengthened with different configurations of CFRP laminates." *Int. J. Current Eng. Technol.*, 2(4), 418–426.

Sebastian, W. M. (2001). "Significance of midspan debonding failure in FRP-plated concrete beams." *J. Struct. Eng.*, 10.1061/(ASCE)0733-9445(2001)127:7(792), 792–798.

Seim, W., Horman, M., Karbhari, V., and Seible, F. (2001). "External FRP poststrengthening of scaled concrete slabs." *J. Compos. Constr.*, 10.1061/(ASCE)1090-0268(2001)5:2(67), 67–75.

Sena-Cruz, J., Barros, J., Coelho, M., and Silva, L. (2012). "Efficiency of different techniques in flexural strengthening of RC beams under monotonic and fatigue loading." *Constr. Build. Mater.*, 29, 175–182.

Shah, A. A., Abbas, H., Alsayed, S. H., Al-Salloum, Y. A., and Almusallam, T. H. (2012). "Predicting residual strength of non-linear ultrasonically evaluated damaged concrete using artificial neural network." *Constr. Build. Mater.*, 29, 42–50.

Smith, S. T., and Kim, S. J. (2009). "Strengthening of one-way spanning RC slabs with cutouts using FRP composites." *Constr. Build. Mater.*, 23(4), 1578–1590.

Smith, S. T., Hu, S., Kim, S. J., and Seracino, R. (2011). "FRP-strengthened RC slabs anchored with FRP anchors." *Eng. Struct.*, 33(4), 1075–1087.

Smith, S. T., and Teng, J. G. (2001). "Interfacial stresses in plated beams." *Eng. Struct.*, 23(7), 857–871.

Smith, S. T., and Teng, J. G. (2002). "FRP-strengthened RC beams I: Review of debonding strength models." *Eng. Struct.*, 24(4), 385–395.

Spadea, G., Swamy, R., and Bencardino, F. (2001). "Strength and ductility of RC beams repaired with bonded CFRP laminates." *J. Bridge Eng.*, 10.1061/(ASCE)1084-0702(2001)6:5(349), 349–355.

Tan, K. Y. (2003). "Evaluation of externally bonded CFRP systems for the strengthening of RC slabs." M.S. thesis, Univ. of Missouri-Rolla, Rolla, MO.

Teng, J. G., Smith, S. T., Yao, J., and Chen, J. F. (2003). "Intermediate crack-induced debonding in RC beams and slabs." *Constr. Build. Mater.*, 17(6–7), 447–462.

Topcu, I. B., and Saridemir, M. (2008). "Prediction of compressive strength of concrete containing fly ash using artificial neural network and fuzzy logic." *Comput. Mater. Sci.*, 41(3), 305–311.

Toutanji, H., Saxena, P., Zhao, L., and Ooi, T. (2007). "Prediction of interfacial bond failure of FRP-concrete surface." *J. Compos. Constr.*, 10.1061/(ASCE)1090-0268(2007)11:4(427), 427–436.

White, T. W., Soudki, K. A., and Erki, M. (2001). "Response of RC beams strengthened with CFRP laminates and subjected to a high rate of loading." *J. Compos. Constr.*, 10.1061/(ASCE)1090-0268(2001)5:3(153), 153–162.

Wu, Z., Islam, S. M., and Said, H. (2009). "A three-parameter bond strength model for FRP-concrete interface." *J. Reinforc. Plast. Compos.*, 28(19), 2309–2323.

Wu, Z. S., and Niu, H. D. (2007). "Prediction of crack-induced debonding failure in R/C structures flexurally strengthened with externally bonded FRP composites." *JSCE J. Mater., Conc. Struct. Pavements*, 63(4), 620–639.

Yalim, B., Kalayci, A. S., and Mirmiran, A. (2008). "Performance of FRP-strengthened RC beams with different concrete surface profiles." *J. Compos. Constr.*, 10.1061/(ASCE)1090-0268(2008)12:6(626), 626–634.

Yao, J., Teng, J. G., and Lam, L. (2002). "Debonding in RC cantilever slabs strengthened with FRP strips." *Proc., Int. Conf. on Advanced Polymer Composites for Structural Applications in Construction*, Southampton Univ., U.K., 125–133.

Yao, J., Teng, J. G., and Lam, L. (2005). "Experimental study on intermediate crack debonding in FRP-strengthened RC flexural members." *Adv. Struct. Eng.*, 8(4), 365–396.

Ye, L. P., Cui, W., and Yue, Q. R. (2001). "Analysis and calculation of flexural strength of RC members strengthened with CFRP sheet." *Build. Struct.*, 35(3), 3–5 (in Chinese).

You, Y., Choi, K., and Kim, J. (2012). "An experimental investigation on flexural behavior of RC beams strengthened with prestressed CFRP strips using a durable anchorage system." *Compos. B Eng.*, 43(8), 3026–3036.

Zhang, G. F., Kishi, N., and Mikami, H. (2003). "Influence of material properties of FRPs on strength of flexural strengthened RC beams." *Proc., 6th Int. Symp. on FRP Reinforcement for Concrete Structures (FRPRCS6)*, World Scientific Publications, Singapore, 327–336.